Green light enabled Staudinger–Bertozzi ligation†

Kubra Kalayci,[ab] Hendrik Frisch,[ab] Christopher Barner-Kowollik *[abc] and Vinh X. Truong *[ab]

We introduce a visible light-induced Staudinger–Bertozzi ligation *via* photo-uncaging of a triphenylphosphine moiety with a photolabile coumarin derivative. Our action plot study examines the conversion as the function of wavelength, revealing that the uncaging process and Staudinger reaction can be triggered by green light ($\lambda < 550$ nm). We further demonstrate the applicability of our approach in materials science *via* endgroup modification of water soluble poly(ethylene glycol) and green light-induced patterning of a solid substrate.

The Staudinger–Bertozzi ligation is among the most widely used coupling chemistries for the modification of naturally occurring biomolecules, enabling the study and manipulation of biological processes.[1,2] This ligation technique involves converting stable azides to amides with the aid of trivalent phosphorus reagents. Compared to other azide selective chemistries, such as the copper-catalysed or strain-promoted azide–alkyne cycloadditions, Staudinger–Bertozzi reactions generally feature slower reaction kinetics and lower efficiency.[3] However, the phosphine probes have higher metabolic stability in biological environments, which affords facile and selective conjugation to the targeted biomacromolecules both *in vivo* and *in vitro*.[4] Thus, despite the emergence of new bioorthogonal coupling chemistries,[5] including the isonitrile and nitrile oxide cycloadditions,[6,7] inverse electron demand Diels–Alder reactions,[8–10] nucleophilic thiol-addition,[11,12] and pentafluorophenyl-based S_NAr reactions,[13–15] the Staudinger–Bertozzi ligation remains an indispensable tool for bioconjugation.[16] Critically, the ligation can be conducted in the presence of living cells without notable toxicity, enabling the modification and labelling of cell surfaces.[17,18] The orthogonality of Staudinger coupling against cellular components further affords *in vivo* attachment of glycans to cell membranes for controlling the extracellular communication.[18]

Applying a light switch to trigger the bioorthogonal ligation on-demand significantly enhances the utility of the labelling process *in situ*, due to the unique spatial and temporal control that light provides.[19] A common strategy to integrate light-responsiveness into the conjugation process is to cage one reactive component with a photoremovable protecting group (PPG) to inhibit its reactivity.[20–22] Upon light irradiation, the protecting group is removed, revealing the reactive moiety. Examples of such photochemical systems include the photo-uncaging of *o*-nitrobenzyl (*o*-NB),[23] coumarin,[24] bimane,[25] and BODIPY[22] for the release of thiol groups, which can participate in the bioorthogonal thiol-Michael addition.

In Staudinger ligations, caging the phosphorus component provides additional protection against spontaneous oxidation. The first report on light-activated Staudinger–Bertozzi ligation employed an *o*-NB as the protecting group, enabling the UV light-induced release of the phosphine probes for labelling of azide-functionalized cell membranes.[26] Moving away from UV light, which can be damaging to biological species, the team of Lam employed anthracene derivatives to cage the triphenylphosphine group.[27,28] These authors demonstrated the triggering of a traceless Staudinger ligation by blue light at $\lambda < 440$ nm. To broaden the utility of the light-induced Staudinger ligation in biology, new photolabile reagents are expected to have both long-wavelength absorption for deep tissue penetration and rapid uncaging for efficient bioconjugation.

Herein, we introduce a strategy to significantly red-shift the activation wavelength employed in photo-triggering the Staudinger–Bertozzi ligation by using a photolabile coumarin moiety for caging of the phosphorus reagent, which can be uncaged by green light ($\lambda < 550$ nm) (Scheme 1). Our strategy was applied to green light-trigger Staudinger ligations for

[a] *Centre for Materials Science, Queensland University of Technology, 2 George Street, Brisbane, QLD 4000, Australia. E-mail: christopher.barnerkowollik@qut.edu.au, vx.truong@qut.edu.au*
[b] *School of Chemistry and Physics, Queensland University of Technology, 2 George Street, Brisbane, QLD 4000, Australia*
[c] *Institute for Nanotechnology, Karlsruhe Institute of Technology (KIT), Hermann-von-Helmholtz-Platz 1, 76344 Eggenstein-Leopoldshafen, Germany*

† Electronic supplementary information (ESI) available. See DOI: https://doi.org/10.1039/d2cc00911k

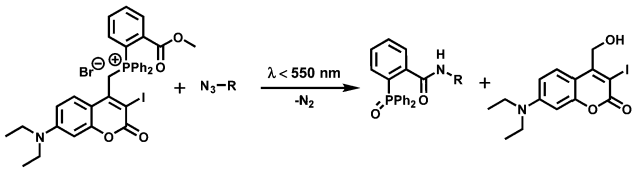

Scheme 1 Green light-induced Staudinger–Bertozzi ligation by caging the phosphorus component with a photolabile coumarin moiety.

efficient end group modification of a water soluble poly(ethylene glycol) (PEG). Further, we demonstrate efficient patterning of a solid substrate by green light irradiation.

We utilise a second-generation coumarinylmethyl photoremovable protecting group, specifically the 7-diethylamino-coumarin-4-methyl (DEACM) moiety, featuring high photouncaging efficiency for the release of various leaving group.[29] Modification of the 3-position of the DEACM moiety with electron-rich donor functions, such as styryl, nitrile or halide further redshift the absorbance and enhance the uncaging efficiency.[30 32] Thus, we synthesised a precursor, 4-(bromomethyl)-7-(diethylamino)-3-iodo-2*H*-chromen-2-one, which can react with the triphenylphosphine component, methyl 2-(diphenylphosphino)benzoate (MPPB) or triphenylphosphine, in a one-step procedure to form the caged compound (ESI,† Section S3.5) in good yields (71–82%). Subsequently, the photo-release of the MPPB was investigated by irradiating the caged MPPB solution in acetonitrile (2.64 mM) at λ = 440 nm wavelength for 30 min, and the products were examined by liquid chromatography-mass spectrometry (LC-MS) (Fig. 1 and Table S1, ESI†). The released phosphine product was identified in the form of the oxidised MPPB (compound **B** in Fig. 1), together with other side products resulting from the photolysis of the DEACM moiety. The photo-uncaging was associated with a change in the solution colour, which may be attributed to the degradation of the iodine-substituted DEACM, resulting in the release of iodine and side products **C**, **D** and **E**. The distorted peaks observed for the side products may be due to the very low concentrations of such species, which are below the data acquisition limit of the UV detector of the HPLC-MS.

Next, we monitored the wavelength dependent photo-release of the MPPB using a monochromatic tunable laser source and analysed the ^{1}H-NMR spectra before and after each irradiation step (Fig. 2 and Fig. S2, ESI†). A 2.64 mM solution of caged MPPB was prepared in $CDCl_3$ and separated into smaller vials. Each sample was irradiated with an identical number of photons (1.3×10^{22} mol) at different wavelengths using a monochromatic light source. Here, the conversion was followed by examining the resonances corresponding to the methyl ester group of the caged compound, compared to the methyl ester group of the oxidised MPPB product (Fig. 2a and Fig. S16, ESI†). Based on the integration of these resonances, we were able to calculate the wavelength dependent conversion of the photochemical release, which is presented as a function of irradiation

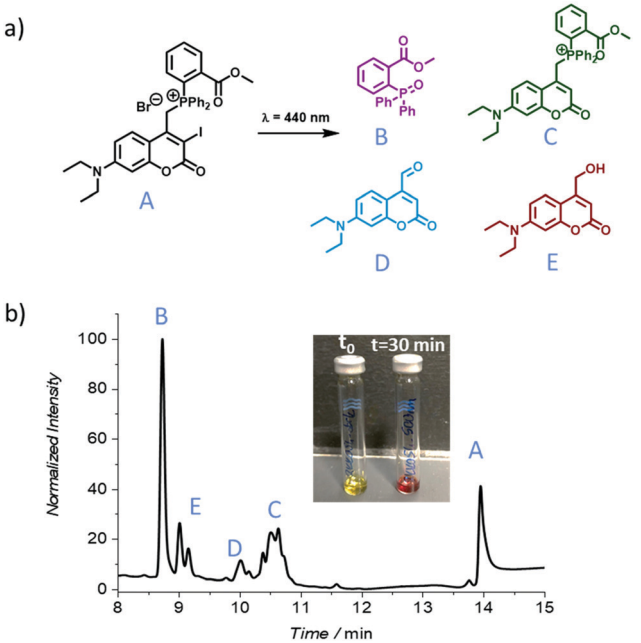

Fig. 1 (a) Photo-release products of caged MPPB identified *via* LC-MS. (b) LC-MS elugram after irradiation at λ = 440 nm (refer to Table S1 (ESI†) for the detailed mass spectrometric analysis). The inset depicts the colour change of the solution from yellow to red after irradiation.

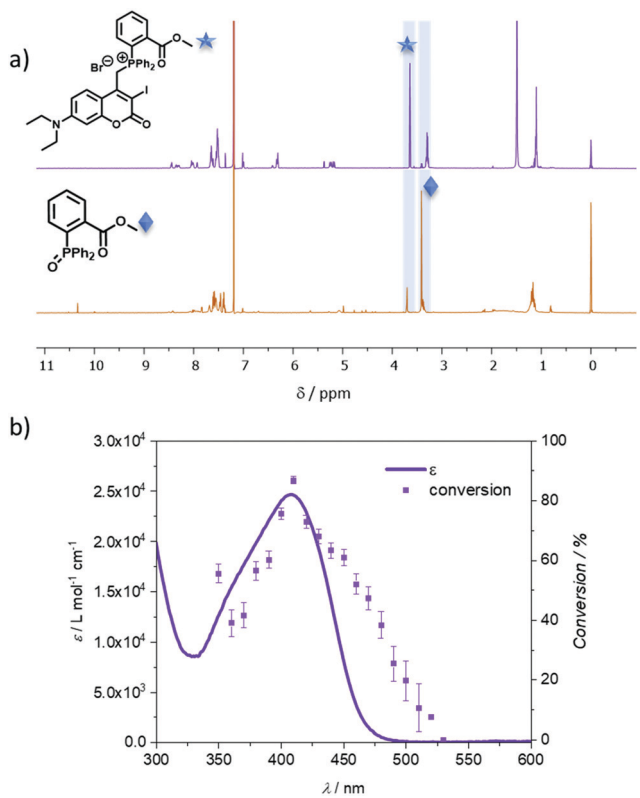

Fig. 2 (a) ^{1}H-NMR spectra before and after irradiation of caged MPPB. The star shape indicates the methyl ester proton resonances of the caged MPPB and the tetragon shape indicates the same proton resonance of the uncaged MPPB (refer to Fig. S13 for complete assignment of the resonances of the NMR spectrum of caged MPPB, ESI†). (b) Action plot[34] and UV-Vis spectrum of the caged MPPB. The conversion is calculated based on the resonances highlighted in ^{1}H-NMR spectra.

wavelength (Fig. 2b). We previously reported that the photo-reactivity of molecules does not necessarily align with their absorption spectra, and in most cases a red-shift in photo-reactivity compared to the absorbance is observed.[33,34] This trend was also observed for the photo-release of MPPB, whereby the conversion occurs at wavelength in the λ = 480–530 nm region, at which the compound only has low extinction coefficients ($\varepsilon \leq 0.8 \times 10^3$ L mol^{-1} cm^{-1}). However, we did not observe a shift between the Abs_{max} and maximum reactivity. Nevertheless, it is noted that although there is a shift in reactivity compared to the absorption spectrum, the reactivity follows the same trend as the absorbance, increasing with increasing absorbance and – after reaching a maximum value – decreasing again. The quantum efficiency of the uncaging process, based on the kinetics of the conversion over time, at λ = 445 nm was calculated to be Φ = 0.035. This value is higher than quantum efficiency of photo-uncaging of the anthracence moiety (Φ = 0.025)[28] at λ = 420 nm. Furthermore, the photolysis occurs with a quantum efficiency Φ = 0.0024 at λ = 505 nm, which is by far the longest wavelength reported for the photouncaging of the MPPB moiety.[28] Additionally, photo-uncaging of triphenylphosphine is highly efficient by blue LED light irradiation, yielding triphenylphosphine oxide with >90% conversion within 15 min (Fig. S3 and S4, ESI†).

Having confirmed the successful uncaging of the MPPB, we subsequently investigated the reactivity of the released MPPB function in conventional Staudinger–Bertozzi ligation, by photo-release of MPPB in the presence of a PEG-azide (Fig. 3a). Specifically, a solution of PEG-azide (10 mM) and caged MPPB (5 molar equivalent) in acetonitrile/H_2O (4/1) mixture was irradiated with a green (λ = 505 nm) LED light source for 30 min under nitrogen atmosphere, and the polymer end group modification was monitored by size exclusion chromatography hyphenated with mass spectrometry (SEC-MS). Analysis of the SEC trace of the polymer product reveals the formation of the ligated amide compound (Fig. 3b). Examining the mass spectrum of this SEC trace reveals the multiple patterns of the PEG repeating units with a difference of m/z = 44.0264, corresponding to the molecular weight of one PEG repeating unit. The obtained m/z values agree well with the simulated isotopic patterns of the PEG amide product. Furthermore, both the ^{1}H and ^{31}P NMR spectra of the polymer product indicate resonances corresponding to the phosphine oxide amide adduct, specifically the aromatic protons between δ = 7–7.5 ppm and the phosphorus resonance at around δ = 35 ppm (Fig. S1, ESI†). Notably, when a caged triphenylphosphine was used instead of caged MPPB, the azide function was converted to an amine following the uncaging process (Fig. S23, ESI†). Our chemical approach therefore can provide a light-induced *in situ* generation of amine functionality, which can be potentially used in bioorthogonal ligation, *e.g. via* reaction with an activated *N*-hydroxysuccinimide ester.[35] The Staudinger reactions did not occur when the reacting mixture (polymer and caged phosphine compound) are left in the dark.

To highlight the spatio-temporal control over the ligation and potential application in materials science, we report the photo-patterning a solid substrate using the light-induced

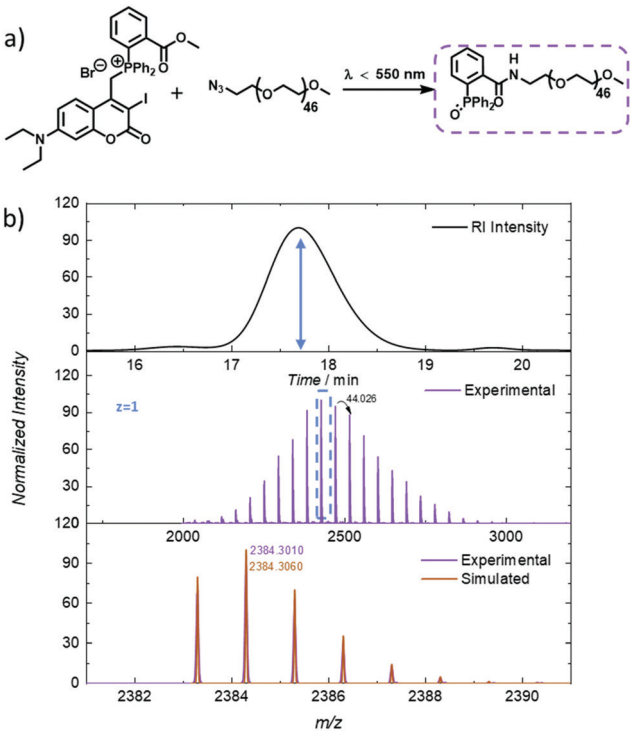

Fig. 3 (a) Photo-controlled Staudinger–Bertozzi ligation with PEG-azide and caged MPPB. (b) SEC-MS analysis of the PEG after irradiation with 505 nm LED. Mass spectrum, specific to the selected peak in the SEC trace showing the clean repeating unit patterns of the modified PEG. Zoomed-in spectra of the experimental results and simulated data overlap precisely.

Staudinger–Bertozzi ligation. Specifically, a silicon wafer was modified with an azide functionalized 3-(triethoxysilyl) propan-1-amine (APTES) (Fig. 4). It was subsequently covered with a photomask and placed in a solution of caged MPPB (c = 2.64 mM), followed by irradiation under either a λ = 445 or 505 nm LED light (Fig. S12, ESI†). Characterisation of the wafer

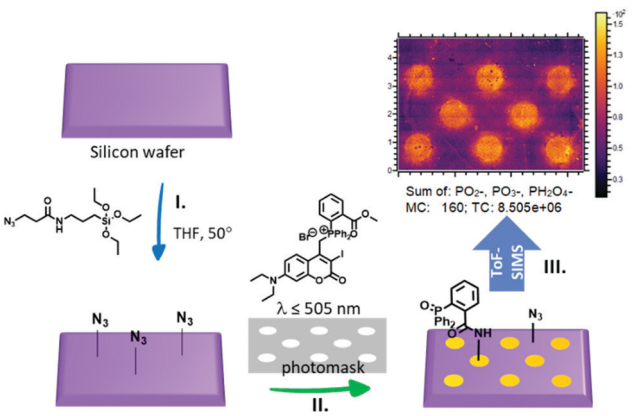

Fig. 4 The strategy for functionalization of a silicon surface by Staudinger–Bertozzi ligation and the ToF-SIMS image of the patterned surface. (I) Functionalization of silicon surface with azide functionalized APTES. (II) Photo-patterning process with caged MPPB using a dotted photomask. (III) ToF-SIMS image of the patterned surface in negative mode. Yellow color represents the sum of ion fragments related to phosphorus.

using Time-of-Flight Secondary Ion Mass Spectrometry (ToF-SIMS) reveals the presence of the phosphorus fragments (Fig. 4 and Fig. S6, ESI†) of the Staudinger ligated product in the irradiated areas. Specifically, the fragments of PO_2^-, PO_3^-, $PH_2O_4^-$ ions display high contrast on the dotted regions, whereas the areas covered with photomask are completely clean from these fragments.

In conclusion, we introduce a photochemical approach to enable control over the Staudinger–Bertozzi ligation using light of wavelengths of up to $\lambda < 550$ nm. To the best of our knowledge, this is the most red-shifted activation wavelength reported to date for the light-induced Staudinger ligation. The products of photorelease were fully identified by LC-MS and the green light-induced Staudinger–Bertozzi ligation was successfully performed for the end group modification of a water-soluble PEG. The utility of our photochemical system in materials engineering was demonstrated by photo-patterning of a solid substrate. We submit that our photochemical approach will significantly enhance the utility of the Staudinger–Bertozzi ligation, which has already established its use in a wide range of applications in synthetic chemistry and cell-based studies.[1]

C. B.-K. acknowledges the Australian Research Council (ARC) for funding in the context of a Laureate Fellowships enabling his photochemical research program. H. F. acknowledges support by the ARC in the form of a DECRA Fellowship. The authors thank Dr Robert Jones (QUT) for assistance with the ToF-SIMS measurements, as well as QUT's Centre for Materials Science for continued support.

Conflicts of interest

There are no conflicts to declare.

Notes and references

1 C. Bednarek, I. Wehl, N. Jung, U. Schepers and S. Brase, *Chem. Rev.*, 2020, **120**, 4301–4354.
2 M. Kohn and R. Breinbauer, *Angew. Chem., Int. Ed.*, 2004, **43**, 3106–3116.
3 F. L. Lin, H. M. Hoyt, H. van Halbeek, R. G. Bergman and C. R. Bertozzi, *J. Am. Chem. Soc.*, 2005, **127**, 2686–2695.
4 N. J. Agard, J. M. Baskin, J. A. Prescher, A. Lo and C. R. Bertozzi, *ACS Chem. Biol.*, 2006, **1**, 644–648.
5 M. A. Azagarsamy and K. S. Anseth, *ACS Macro Lett.*, 2013, **2**, 5–9.
6 V. X. Truong, K. Zhou, G. P. Simon and J. S. Forsythe, *Macromol. Rapid Commun.*, 2015, **36**, 1729–1734.
7 H. Stöckmann, A. A. Neves, S. Stairs, K. M. Brindle and F. J. Leeper, *Org. Biomol. Chem.*, 2011, **9**, 7303–7305.
8 M. L. Blackman, M. Royzen and J. M. Fox, *J. Am. Chem. Soc.*, 2008, **130**, 13518–13519.
9 B. L. Oliveira, Z. Guo and G. J.-L. Bernardes, *Chem. Soc. Rev.*, 2017, **46**, 4895–4950.
10 J. Carthew, J. E. Frith, J. S. Forsythe and V. X. Truong, *J. Mater. Chem. B*, 2018, **6**, 1394–1401.
11 C. T. Huynh, F. Liu, Y. Cheng, K. A. Coughlin and E. Alsberg, *ACS Appl. Mater. Interfaces*, 2018, **10**, 25936–25942.
12 V. X. Truong, I. Donderwinkel and J. E. Frith, *J. Polym. Sci., Part A: Polym. Chem.*, 2019, **57**, 1872–1876.
13 A. P.-P. Kröger, J.-W. D. Paats, R. J.-E. A. Boonen, N. M. Hamelmann and J. M.-J. Paulusse, *Polym. Chem.*, 2020, **11**, 6056–6065.
14 J. Engelke and V. X. Truong, *Polym. Chem.*, 2020, **11**, 7015–7019.
15 G. Delaittre and L. Barner, *Polym. Chem.*, 2018, **9**, 2679–2684.
16 S. S. van Berkel, M. B. van Eldijk and J. C. van Hest, *Angew. Chem., Int. Ed.*, 2011, **50**, 8806–8827.
17 E. B. Saxon and C. R. Bertozzi, *Science*, 2000, **287**, 2007.
18 J. A.-D. H.-D. Prescher, D. H. Dube and C. R. Bertozzi, *Nature*, 2004, **430**, 873.
19 J. Li, H. Kong, C. Zhu and Y. Zhang, *Chem. Sci.*, 2020, **11**, 3390–3396.
20 G. C. Ellis-Davies, *Nat. Methods*, 2007, **4**, 619–628.
21 V. X. Truong, *ChemPhotoChem*, 2020, **4**, 564–570.
22 M. Li, A. P. Dove and V. X. Truong, *Angew. Chem., Int. Ed.*, 2020, **59**, 2284–2288.
23 N. Kotzur, B. Briand, M. Bayermann and V. Hagen, *J. Am. Chem. Soc.*, 2009, **131**, 16927–16931.
24 M. M. Mahmoodi, S. A. Fisher, R. Y. Tam, P. C. Goff, R. B. Anderson, J. E. Wissinger, D. A. Blank, M. S. Shoichet and M. D. Distefano, *Org. Biomol. Chem.*, 2016, **14**, 8289–8300.
25 V. X. Truong, F. Li and J. S. Forsythe, *Biomacromolecules*, 2018, **19**, 4277–4285.
26 L. Shah, S. T. Laughlin and I. S. Carrico, *J. Am. Chem. Soc.*, 2016, **138**, 5186–5189.
27 P. Hu, T. Feng, C. C. Yeung, C. K. Koo, K. C. Lau and M. H. Lam, *Chemistry*, 2016, **22**, 11537–11542.
28 P. Hu, K. Berning, Y. W. Lam, I. H. Ng, C. C. Yeung and M. H. Lam, *J. Org. Chem.*, 2018, **83**, 12998–13010.
29 P. Klán, T. Šolomek, C. G. Bochet, A. Blanc, R. Givens, M. Rubina, V. Popik, A. Kostikov and J. Wirz, *Chem. Rev.*, 2013, **113**, 119–191.
30 X. J. Tang, Y. Wu, R. Zhao, X. Kou, Z. Dong, W. Zhou, Z. Zhang, W. Tan and X. Fang, *Angew. Chem., Int. Ed.*, 2020, **59**, 18386–18389.
31 Q. Lin, L. Yang, Z. Wang, Y. Hua, D. Zhang, B. Bao, C. Bao, X. Gong and L. Zhu, *Angew. Chem., Int. Ed.*, 2018, **57**, 3722–3726.
32 L. Josa-Culleré and A. Llebaria, *ChemPhotoChem*, 2021, **5**, 296–314.
33 K. Kalayci, H. Frisch, V. X. Truong and C. Barner-Kowollik, *Nat. Commun.*, 2020, **11**, 4193.
34 I. M. Irshadeen, S. L. Walden, M. Wegener, V. X. Truong, H. Frisch, J. P. Blinco and C. Barner-Kowollik, *J. Am. Chem. Soc.*, 2021, **143**, 21113–21126.
35 V. X. Truong and C. Barner-Kowollik, *ACS Macro Lett.*, 2021, **10**, 78–83.